Design and Performance Estimates of an Ablative Gallium Electromagnetic Thruster

Robert E. Thomas
NASA Glenn Research Center, Cleveland, OH 44135
Email: Robert.E.Thomas@nasa.gov

Abstract

The present study details the high-power condensable propellant research being conducted at NASA Glenn Research Center. The gallium electromagnetic thruster is an ablative coaxial accelerator designed to operate at arc discharge currents in the range of 10-25 kA. The thruster is driven by a four-parallel line pulse forming network capable of producing a 250 μs pulse with a 60 kA amplitude. A torsional-type thrust stand is used to measure the impulse of a coaxial GEM thruster. Tests are conducted in a vacuum chamber 1.5 m in diameter and 4.5 m long with a background pressure of 2 μtorr. Electromagnetic scaling calculations predict a thruster efficiency of 50% at a specific impulse of 2800 seconds.

Nomenclature

e = Electron charge, C
E = Discharge energy, J
I_b = Impulse bit, N-s
J = Discharge current, A
k = Boltzmann's constant, J/K
k_s = Spring constant, kg/s^2
L = Inductance, H
m_b = Mass bit, kg
r_a/r_c = Anode to cathode radius ratio, m
T = Thrust, N
T_e = Electron temperature, eV
V = Voltage, V
Z = Ionic charge state
u_e = Exhaust velocity, m/s
μ_o = Vacuum permittivity, H/m
GEM = Gallium electromagnetic
PFN = Pulse forming network
MPDT = Magnetoplasmadynamic thruster

Introduction

Magnetoplasmadynamic thrusters (MPDTs) are electromagnetic accelerators capable of providing a high thrust density over a wide range of exhaust velocities, making them potentially attractive candidates for lunar and Mars cargo missions. Unfortunately, erosion of the central cathode severely limits the lifetime of the thrusters [1]. Additionally, poor thruster efficiences ($< 40\%$) have traditionally been obtained in the specific impulse (I_{sp}) ranges of interest. The gallium electromagnetic (GEM) thruster [2-6] was conceived to address these two issues. The GEM thruster is a quasi-steady, coaxial accelerator that utilizes ablated cathode mass for propellant. The thruster is currently designed to operate in a self-field mode (no applied magnetic field) with arc discharge currents on the order of 10-25 kA. The thruster exploits cathode ablation, inherent in MPDTs, to create microsecond time-scale injection of propellant mass and significantly increase thruster lifetime. A photograph of a 20 J laboratory model is shown in Fig. 1. The thruster is designed to ablate a thin layer of liquid gallium that is continuously fed through the porous central electrode. Electrode erosion is treated as an integral aspect of operation rather than a unavoidable, detrimental side effect.

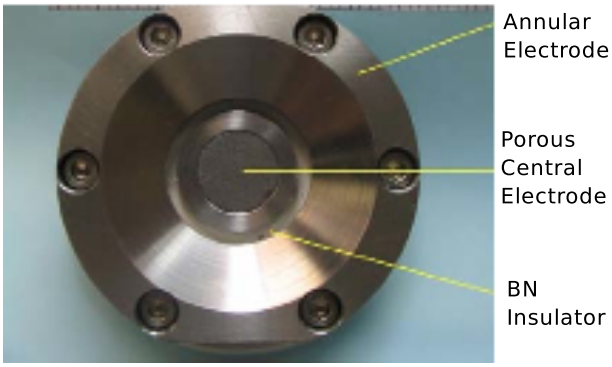

Figure 1: Low-energy breadboard model utilizing a sintered tungsten porous cathode [3].

The advantages of using gallium as a propellant include:

1. *Storability*: Gallium has a density of 5.99 g/cm^3 and a melting point of 30 °C. It can be stored

as a solid and melted into a liquid with minimal thermal management.

2. *Propellant Feeding*: Liquid gallium can be fed to the thruster through the use of mechanically robust electromagnetic pumps. This reduces the number of moving parts and eliminates the need for pulsed gas valves.

3. *Ground Based Testing*: Gallium is non-toxic, relatively inexpensive, and can be pumped (condensed) on a cooled baffle, which significantly reduces facility requirements and costs.

4. *Ionization*: The first ionization potential of gallium is only 5.99 eV, minimizing frozen flow losses, which are the major loss mechanism for MW-level MPDTs.

The present study discusses the ongoing high-power, condensible propellant MPDT research at NASA Glenn Research Center. A description of the thruster, pulse forming network, and thrust stand is presented. Electromagnetic scaling relations are then discussed, and calculations of the thruster efficiency and specific impulse are given.

Apparatus

GEM Thruster

A photograph of the GEM thruster is shown in Fig. 2. The annular anode has an inner diameter of 25.5 mm. The 8.5 mm diameter gallium electrode (99.999% purity) is electrically insulated from the outer electrode by boron nitride. Tests will be completed using both flat-tip and conical-tip gallium electrodes. The baseline configuration to be tested is an anode-to-cathode radius ratio of $r_a/r_c = 3$. Several annular electrodes have been fabricated that will permit testing of electrode radius ratios of 3, 5, 7, and 10.

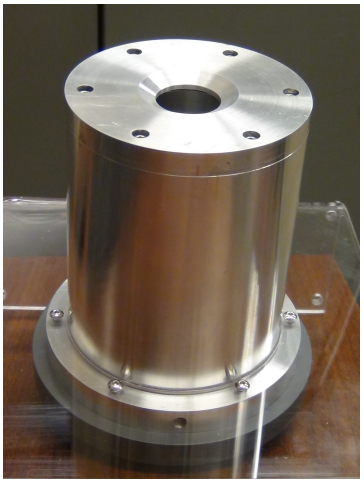

Figure 2: Photograph of 8.9 cm O.D. GEM thruster.

It should be noted that while a flight-like model will utilize a porous central electrode that is continuously replenished with liquid propellant (akin to Fig. 1), a solid gallium cathode is used in the present experiments. This is done to obtain accurate measurements of the mass ablated per pulse (mass bit). The energy required to melt solid gallium (0.06 eV/atom) is much less than the heat of vaporization (2.6 eV/atom), so the phase difference is not expected to alter the performance of the thruster.

Vacuum Facility and Thrust Stand

Tests are conducted at NASA GRC vacuum facility 3 (VF-3), which has a diameter of 1.5 m and is 4.5 m in length. The chamber is evacuated by four oil diffusion pumps with a background pressure of 2 μtorr prior to each thruster shot.

A torsional-type thrust stand is used to perform impulse measurements [7]. The impulse is determined in terms of the thrust stand deflection x, spring stiffness k, and natural frequency ω_n

$$I_b = \frac{k_s x}{\omega_n} \tag{1}$$

In practice x is measured as the maximum deflection of the thrust stand after an impulse is applied, k is determined by exerting a known force and observing the deflection, and ω_n is determined by counting the undamped frequency of the thrust stand oscillation. In-sitsu calibration weights are used to apply a known force to determine the deflection of the thrust stand. The stand has a 2% uncertainty in the impulse-bit measurement. Fig. 3 shows a a schematic of the thrust stand and Fig. 4 shows photograph of the thruster mounted on the stand.

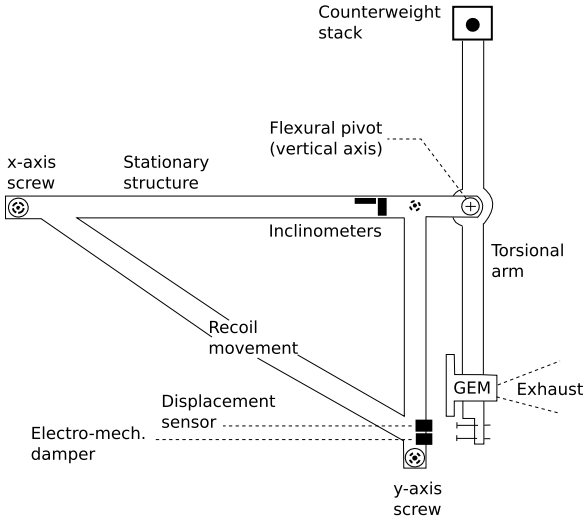

Figure 3: Top view schematic of thrust stand [7].

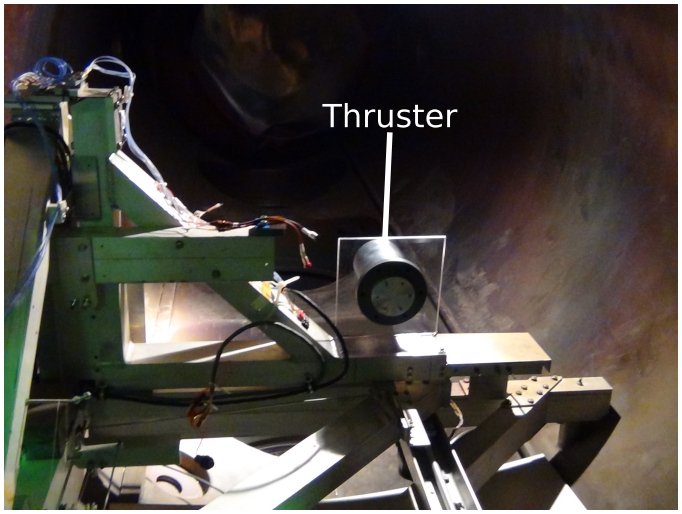

Figure 4: GEM thruster mounted on thrust stand. A polycarbonate mounting plate electrically isolates the thruster from the thrust stand.

Pulse Forming Network

The GEM thruster is powered by a four parallel line pulse forming network (PFN). Each line consists of six $C = 600$ μF capacitors charged to a maximum of 800 V, yielding a total of 24 capacitors and a bank energy of 4.6 kJ. The $L = 400$ nH coiled inductors are constructed of 10 gauge magnet wire. The PFN impedance is $(L/C)^{1/2}/4 = 6.5$ mΩ, which is designed to match the thruster impedance. This eliminates the need for a matching resistor and maximizes the energy transferred to the thruster. A copper sheet with punched holes is laid over the capacitors to provide a common ground (ground plane) as shown in Fig. 5. The PFN is mounted adjacent to VF-3 to minimize parasitic effects within the transmission lines. The PFN is capable of providing 60 kA discharge currents for a duration of 250 μs. A numerically simulated discharge current waveform for a charging voltage of 300 V is shown in Fig. 6. A low-energy spark igniter mounted inside VF-3 is used to discharge the capacitors (similar to a pulsed plasma thruster). A schematic showing electrically the PFN, igniter, and thruster is shown in Fig. 7.

Thruster Performance

The discharge current, arc voltage (electric potential across thruster electrodes during current pulse), mass bit, and impulse bit are directly measured and can be used to characterize the thruster performance. The specific impulse is found though $I_{sp} = I_b/m_b$. The impulsive efficiency is calculated using

$$\eta = \frac{I_b^2}{2m_b E} \tag{2}$$

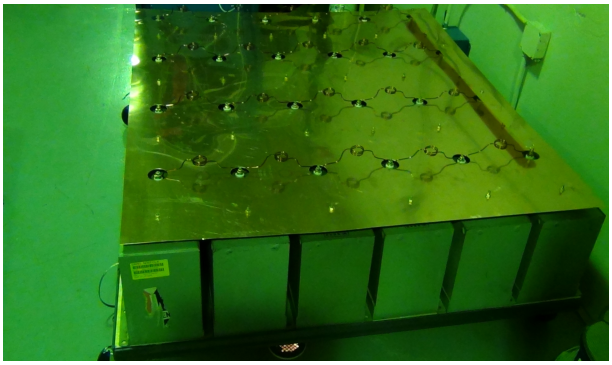

Figure 5: Side view of the six-ladder, four parallel line pulse forming network.

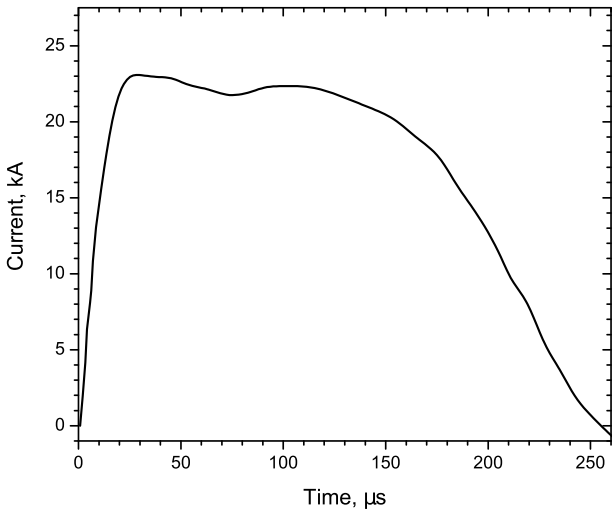

Figure 6: Simulated discharge current pulse for a charging voltage of 300 V.

where the discharge energy is found through

$$E = \int V_{arc}(t) J(t)\ \mathrm{d}t \tag{3}$$

An effective thrust and mass flow rate can be calculated from the impulse and mass bit by defining a quasi-steady time duration [8]

$$\Delta t = \frac{\int J^2(t)\ \mathrm{d}t}{< J >^2} \tag{4}$$

where $< J >$ is the quasi-steady current, averaged between 20-140 μs for the pulse shown in Fig. 6. Dividing each term in Eqn. (2) by (4), one arrives at the familiar form for the thruster efficiency

$$\eta = \frac{T^2}{2\dot{m}P} = \frac{T^2}{2\dot{m}JV_{arc}} \tag{5}$$

The following paragraphs provide analytical expressions for the thrust, arc voltage, and thruster efficiency. These calculations were used to design the thruster and to provide insight on the major energy loss mechanisms. Prior experimental data is used to estimate some of the necessary input parameters.

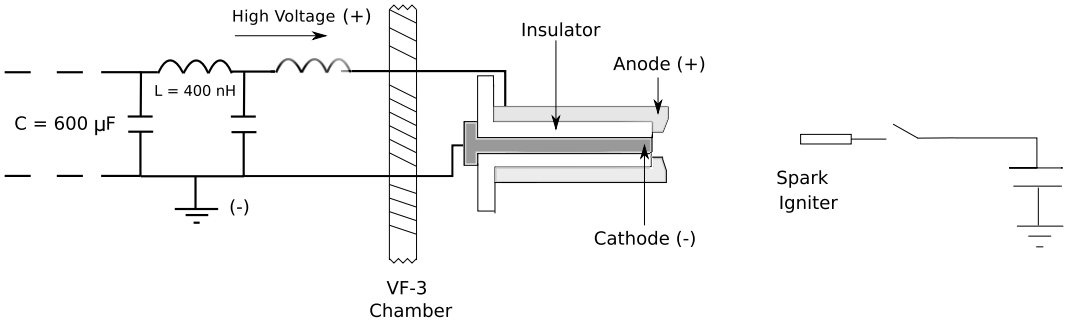

Figure 7: Electrical schematic of the pulse forming network and pulse igniter.

Prior GEM thruster experiments have shown that the mass ablated per pulse scales quadratically with the discharge current $\dot{m} \propto J^2$ [6]. This yields an exhaust velocity (and efficiency) that is invariant with input power. This can be seen through the examination of thrust and exhaust velocity relations for a coaxial electromagnetic accelerator [9]

$$T = \frac{1}{2}L'J^2, \text{where } L' = \frac{\mu_o}{2\pi}\left(\ln\frac{r_a}{r_c} + \frac{3}{4}\right) \quad (6)$$

$$u_e = \tfrac{1}{2}L'\frac{J^2}{\dot{m}} \quad (7)$$

Therefore, in order to increase the performance of the thruster it is necessary to increase the inductance gradient L'. This is accomplished by increasing the anode to cathode radius ratio r_a/r_c. Efficiency predictions using r_a/r_c as a variable can be made through the use of Eqns. (5), (6), and (8). The arc voltage is the sum of the electromagnetic, electrothermal (heating and ionization), and the sheath voltage contributions

$$V_{arc} = \frac{T^2}{2\dot{m}J} + \frac{\dot{m}(Ze\sum\epsilon_i + 3/2kT_e)}{Jm_{ion}} + V_{sheath} \quad (8)$$

where ϵ_i is the ionization potential in eV and m_{ion} is the ion mass. The first, second, and third ionization potentials for gallium are 6, 20.5, and 30 eV. The electron temperature T_e is taken to be 4 eV, which has been found experimentally using Langmuir probes. Ionization calculations within the inter-electrode region yield $Z = 2{-}3$. A sheath voltage of 30 V is used, which is estimated by extrapolating a previously obtained $V_{arc} - J$ curve to zero discharge current [4]. The calculated performance is shown in Figs. 8 and 9, for a fixed discharge current of 23 kA. The power during the quasi-steady portion of the pulse is calculated to be 4.5 MW, yielding a thrust-to-power ratio of 36 N/MW. The corresponding thrust density is 2.6×10^4 N/m^2.

A summary of MPDT performance [8-12] is shown in Table 1 for various propellants. It can

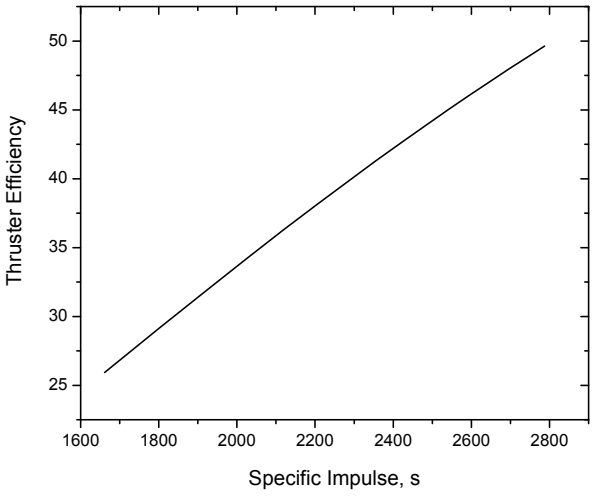

Figure 8: Estimated thruster efficiency vs. specific impulse for $3 < r_a/r_c < 10$. At an electrode radius ratio of 10, the efficiency is 50% at an I_{sp} of 2800 s.

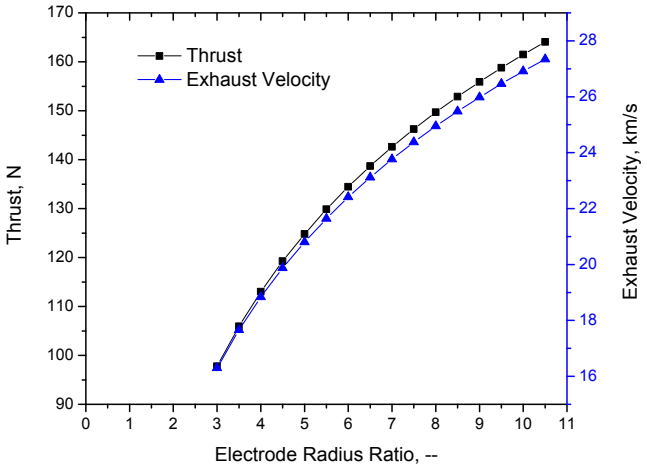

Figure 9: Estimated thrust and exhaust velocity as a function of electrode radius ratio.

be seen that the GEM thruster efficiency compares favorably with prior MPDT research, with an I_{sp} in the moderate range of 3000 s. Further increases in efficiency (>50%) may be possible through the optimized use of applied magnetic fields [13].

Table 1: Comparison of MPDT performance with various propellants.

Propellant	Prop. Inj.	Isp, sec	Efficiency
H_2	Gas-fed	10,000	55
Li	Vapor-fed	6,000	50
C_2	Ablation	5,000	19
Teflon	Ablation	1,400	25
Ga	Ablation	2,800	50

Testing Plan

Hardware fabrication is complete and testing is currently underway to ascertain the influence of electrode geometry on ablative thruster performance. As shown in Table 2, testing will be conducted in the 10-25 kA discharge current range, with $r_a/r_c = 3$-10. At lower power levels, anode sheath losses are anticipated (Eqn. 8) to be the major loss mechanism, while frozen flow losses may dominate at higher current levels. Emission spectroscopy will be used to characterize the ionization losses. The use of a low-strength applied field perpendicular to the anode may reduce sheath losses at the lower power levels [14].

Table 2: Testing plan for GEM thruster.

Current	r_a/r_c	r_a/r_c	r_a/r_c	r_a/r_c
10	3	5	7.5	10
15	3	5	7.5	10
20	3	5	7.5	10
25	3	5	7.5	10

Summary

High-power MPDT research utilizing gallium as a propellant has been described. The GEM thruster is a MW-level ablative accelerator designed to mitigate the life-limiting cathode erosion inherent in MPDTs. The experimental apparatus has been described, which includes the thruster, PFN, and thrust stand. Utilizing a thruster with an electrode radius ratio of 10 yields an estimated thrust-to-power ratio of 36 N/MW. Efficiency calculations predict a thruster efficiency of 50% at a specific impulse of 2800 s. Testing is currently underway to validate these predictions.

References

[1] Sovey, J. S. and Mantenieks, M., "Performance and Lifetime Assessment of Magnetoplasmadynamic Arc Thruster Technology," *Journal of Propulsion and Power*, Vol. 7, No. 1, 1991, pp. 71–83.

[2] Polzin, K., Markusic, T., Burton, R., Thomas, R., and Carroll, D., "Gallium Electromagnetic (GEM) Thruster Concept and Design," *42nd AIAA/ASME/SAE/ASEE Joint Propulsion Conference*, Sacramento, CA, July 9-12 2006, AIAA-2006-4652.

[3] Thomas, R., Burton, R., Glumac, N., and Polzin, K., "Preliminary Spectroscopic Measurements for a Gallium Electromagnetic (GEM) Thruster," *43rd AIAA/ASME/SAE/ASEE Joint Propulsion Conference*, Cincinnati, OH, July 8-11 2007, AIAA-2007-5855.

[4] Thomas, R., Burton, R., and Polzin, K., "Preliminary Development and Testing of a Self-Injecting Gallium MPD Thruster," *44th AIAA/ASME/SAE/ASEE Joint Propulsion Conference*, Hartford, CT, July 21-23 2008, AIAA-2008-5081.

[5] Thomas, R., Burton, R., and Polzin, K., "Gallium Electromagnetic (GEM) Thruster Performance Measurements," *31st International Electric Propulsion Conference*, Ann Arbor, MI, Sept. 20-24 2009, IEPC-2009-233.

[6] Thomas, R., Burton, R., and Polzin, K., "Investigation of a Gallium MPD Thruster with an Ablating Cathode," *46th AIAA/ASME/SAE/ASEE Joint Propulsion Conference*, Nashville, TN, Julay 25-28 2010, AIAA-2010-6529.

[7] Haag, T. W., "Thrust Stand for Pulsed Plasma Thrusters," *Review of Scientific Instruments*, Vol. 68, No. 5, 1997, pp. 2060–2067.

[8] Choueiri, E. and Ziemer, J., "Quasi-Steady Magnetoplasmadynamic Thruster Performance Database," *Journal of Propulsion and Power*, Vol. 17, No. 5, 2001, pp. 967–976.

[9] Jahn, R. G., *Physics of Electric Propulsion*, McGraw-Hill Book Company, 1968.

[10] Paccani, G., Chiarotti, U., and Deininger, W., "Quasisteady Ablative Magnetoplasmadynamic Thruster Performance with Different Propellants," *Journal of Propulsion and Power*, Vol. 14, No. 2, 1998, pp. 254–60.

[11] Ducati, A. and Jahn, R., "Investigation of Pulsed Quasi-Steady MPD Arc Jets," Tech. rep., NASA Langley Research Center, 1971.

[12] Polk, J., Tikhonov, V., Semenikhin, S., and Kim, V., "Cathode Temperature Reduction by Addition of Barium in High- Power Lithium Plasma Thrusters," *AIP Conference Proceedings*, Vol. 504, 2000, p. 1556.

[13] Kodys, A. and Choueiri, E., "A Critical Review of the State-of-the-Art in the Performance of Applied-Field Magnetoplasmadynamic Thrusters," *41st AIAA/ASME/SAE/ASEE Joint Propulsion Conference*, 2005, AIAA-2005-4247.

[14] Hoyt, R. P., Scheuer, J. T., Schoenberg, K. F., Gerwin, R. A., Moses, R. W., Henins, I., Black, D. C., and Mayo, R. M., "Optimization of Magnetic Nozzles for Coaxial Plasma Thrusters," *ASME, SAE, and ASEE, Joint Propulsion Conference and Exhibit*, 1994, AIAA-1994-2992.